12-1-2016

What Determines the Fate of Rising Parcels in a Heterogeneous Environment?

Maren Brast
University of Cologne, brast@meteo.uni-koeln.de

Roel A.J. Neggers
University of Cologne

Thijs Heus
Cleveland State University, t.heus@csuohio.edu

AGU PUBLICATIONS

Journal of Advances in Modeling Earth Systems

RESEARCH ARTICLE

10.1002/2016MS000750

What determines the fate of rising parcels in a heterogeneous environment?

Maren Brast[1,2], Roel A. J. Neggers[1], and Thijs Heus[3]

[1]Institute for Geophysics and Meteorology, University of Cologne, Cologne, Germany, [2]Geoverbund ABC/J, Universität zu Köln, Köln, Germany, [3]Department of Physics, Cleveland State University, Cleveland, Ohio, USA

Key Points:
- A rising parcel model is confronted with heterogeneous profiles as sampled from an LES of shallow cumulus
- The impact of the local environment alone can explain much of the variation in parcel termination heights
- Parcel screening inside cumulus clouds can be effective in enabling parcels to reach greater heights

Correspondence to:
M. Brast,
brast@meteo.uni-koeln.de

Citation:
Brast, M., R. A. J. Neggers, and T. Heus (2016), What determines the fate of rising parcels in a heterogeneous environment?, *J. Adv. Model. Earth Syst.*, *8*, 1674–1690, doi:10.1002/2016MS000750.

Received 5 JUL 2016
Accepted 6 OCT 2016
Accepted article online 11 OCT 2016
Published online 24 OCT 2016

Abstract We investigate the potential impact of the local environment on rising parcels in a convective boundary layer. To this end, we use data from an LES simulation of a shallow convective cloud field to feed a parcel model with a range of different local environments, representative of the heterogeneous environment inside a shallow cumulus cloud layer. With this method we can study the statistics of an ensemble of rising parcels, but also the behavior of individual parcels. Through the use of a heterogeneous environment, the interactions between different parcels are indirectly represented. The method, despite its simplicity, allows closer investigation of mechanisms like parcel screening and buoyancy sorting that have frequently been proposed in cumulus parameterization. The relative importance of the entrainment formulation can be assessed, considering various classic entrainment formulations. We found that while the entrainment formulation does affect parcel behavior, the impact of the local environment is significantly more important in determining the eventual fate of the parcel. Using a constant entrainment rate can already explain much of the variation in termination heights seen in nature and LES. The more complex entrainment models then seem to act on top of this mechanism, creating second-order adaptations in the main distribution as established by the heterogeneity of the environment. A parcel budget analysis was performed for two limit cases, providing more insight into the impact of the local environment on parcel behavior. This revealed that parcel screening inside cumulus clouds can be effective in enabling parcels to reach greater heights.

1. Introduction

The representation of moist convective processes in global weather and climate models relies on parameterization. The improvement of convective parameterizations is necessary, but difficult to achieve because many processes are not yet fully understood. One such process is the mixing between parcels and their environment [e.g., *Romps and Kuang*, 2010; *Dawe and Austin*, 2013]. This mixing affects the effective vertical transport of heat, humidity, and momentum. It affects the radiation budget directly through the vertical distribution of strong greenhouse gases (e.g., water vapor), and indirectly through cloud generation and maintenance. The closure for the mixing process is important, since the representation of convection heavily affects both future climate uncertainty and the skill of numerical weather predictions [e.g., *Tiedtke*, 1989; *Vial et al.*, 2013]. This has motivated intense scientific research into mixing and entrainment, which has been ongoing for decades [e.g., *Simpson and Wiggert*, 1969; *Lin*, 1999; *Gregory*, 2001; *De Rooy and Siebesma*, 2010; *Romps and Kuang*, 2010; *Dawe and Austin*, 2013; *De Rooy et al.*, 2013; *Tian and Kuang*, 2016]. Different methods to study entrainment have been used, e.g., analyzing observational data [*Jonas*, 1990] or, more recently, using large-eddy simulations (LES) [*Dawe and Austin*, 2013; *Tian and Kuang*, 2016]. Various different approaches have been proposed to parameterize entrainment (for a recent review see *De Rooy et al.* [2013]). For parameterization schemes of convection in large-scale models the debate of the proper closure for the mixing process is still ongoing [e.g., *Lin*, 1999; *Neggers et al.*, 2002; *Siebesma et al.*, 2003; *Romps and Kuang*, 2010]. The character of the entrainment parameterization depends greatly on the exact definition of the rising parcel. If the approach assumes a bulk parcel, the entrainment formulation should represent the mean entrainment of the population of cloud sizes. On the other hand, when a single parcel is assumed, this parcel represents a single cloud or even a subcloud parcel, rising inside a cumulus cloud. The mixing then represents something very different.

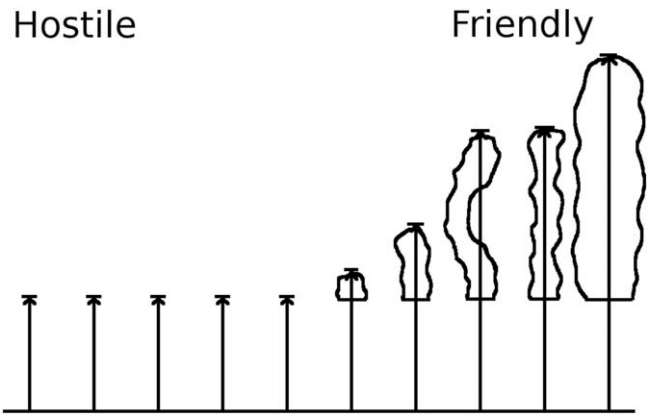

Figure 1. Schematic of rising parcels interacting with the local environment. Parcels within a hostile environment stop near cloud base (left side), while parcels within a friendly environment rise higher (right side).

This study focuses on the entrainment of single rising parcels, and not on the bulk entrainment of a whole ensemble of parcel. An idealized picture of a rising parcel assumes that the parcel ascends through a clean, cloud-free environment. The reality is very different, since a parcel can meet a variety of conditions and states, e.g., it can encounter older, decaying clouds (e.g., pulsating growth [*Heus et al*., 2009]). In case of lateral entrainment, the local environment which the parcel encounters on its way will codetermine how far the parcel will eventually rise. The other factor determining the parcel termination height is the behavior of the entrainment process, affecting the amount of entrained air. A priori, it is not clear which factor will dominate. On the one hand, the local environment can reflect many states. An "unfortunate" parcel, encountering a lot of dry cloud-free air on its way up, will not rise far, while a "fortunate" parcel, rising inside a cumulus cloud, can be expected to be screened off from hostile environment, thus perhaps having a better chance to rise far. The schematic in Figure 1 shows this concept. On the other hand, an entrainment model can interfere with this process, by imposing other dependencies on different variables. Some studies have proposed to represent this "chance effect" of entrainment events by means of a random entrainment (an example for a stochastic model is given in *Romps and Kuang* [2010]). However, one wonders if this stochastic effect should then not rather be represented in the air that is entrained (the source), not in the entrainment model itself. Thus, the resulting question is: To what extent is the fate of the parcel determined by the local environment that it happens to meet on its way, and to what extent is it determined by the entrainment?

The aim of this study is to shed light on this problem, and to determine which factor effectively determines the fate of a rising parcel. To do so, we try to separate between the impact of the local environment and that of the entrainment model itself. While some recent studies have intercompared different entrainment models [e.g., *Chikira and Sugiyama*, 2010], this separation has received less attention. Many entrainment studies are diagnostic in nature, extracting a relation from data, but refraining from investigating its impact on actual parcel behavior. In this study, different entrainment models are tested in one single rising parcel model. The classic and often-applied rising parcel model by *Simpson and Wiggert* [1969, hereinafter SW69] is used for this purpose. The parcel model is fed with a variety of local environments as sampled from an LES of a subtropical marine trade-wind cumulus cloud field. These local environments may represent (i) dry cloud-free conditions, (ii) cumulus clouds, (iii) or any state in between, including partially cloudy conditions. This way, the variability in thermodynamic states typical of a shallow cumulus cloud layer is fed to the rising parcel model. The next step is then to test various entrainment models as proposed in the literature, including dependencies on height, vertical velocity, buoyancy, and stochastics. The constant entrainment rate model is used as a limit case, allowing assessment of the impact of purely the different environments on the rising parcel.

In section 2, a brief review of different entrainment models is provided. In section 3 the parcel model is then formulated, and the experiment setup is described. Section 4 presents the results, followed by a discussion and summary of the findings in section 5.

2. A Short Review of Entrainment Models

In any investigation of the behavior of rising parcels, the entrainment process should play a central role. Since entrainment is difficult to measure, LES simulations of case studies are often used to design parameterizations of entrainment. In the literature, many different entrainment closures have been proposed,

Table 1. Entrainment Formulations From the Literature

Reference	Entrainment Formulation
Simpson and Wiggert [1969]	$0.2/R$
Siebesma et al. [2003]	$1/z$
Soares et al. [2004]	$c\left(\frac{1}{z+\Delta z}+\frac{1}{(z_i-z)+\Delta z}\right)$
Neggers et al. [2002]	$\eta/(\tau w)$
Lin [1999]	λB^{α}

featuring dependencies on a variety of variables (for a review see *De Rooy et al.* [2013]), for both plumes and parcels (from now on we will use the term "parcel," see also section 3.1). An overview of some of the better known formulations is given in Table 1.

Based on laboratory and analytical considerations, SW69 hypothesized that the entrainment should be inversely related to the radius of the cloud R, with ε the fractional entrainment rate. For simplicity, they assume the radius of the cloud to be constant with height. *Tiedtke* [1989] use the same parameterization and assume an average cloud radius to get a constant entrainment rate, differentiating only between two different cumulus cloud regimes.

Another approach is to relate entrainment rate to height. *Siebesma et al.* [2003] found in LES studies that entrainment is decreasing with height. They use this dependency to formulate the entrainment as inversely proportional to the height above the surface z. *Soares et al.* [2004] use a slightly more complex parameterization based on LES results, where entrainment is dependent not only on height but also on boundary layer height z_i, with $c = 0.5$ and Δz the vertical grid spacing, whereas *Siebesma et al.* [2007] use a similar parameterization with a value of $c = 0.4$.

Neggers et al. [2002] proposed an inverse dependency on the vertical velocity of the rising parcel w, featuring a turnover scale τ. τ is argued to represent the typical lifetime of a rising parcel, found to be 400 s based on LES results. With this formulation, parcels with a high vertical velocity have a low entrainment rate, enabling them to rise high.

The buoyancy sorting concept used as a parameterization scheme for shallow cumulus in *Kain and Fritsch* [1990] sees the cloud edge not strictly as cloudy or noncloudy air. Eddies disturb the cloud edge, creating different mixtures of cloudy and noncloudy air. Depending on the fraction of cloudy air in the mixture, the buoyancy of these mixtures differs. Mixtures with a high percentage of environmental air have a negative buoyancy, while mixtures with mostly cloudy air have a positive buoyancy compared to the environment undisturbed by clouds. Positively buoyant mixtures are assumed to entrain into the cloud, while negatively buoyant mixtures detrain from the cloud. To determine the threshold between positively and negatively buoyant mixtures, a critical mixing fraction is calculated taking into account environmental factors such as temperature and humidity. This model was further developed and applied by *Bretheron et al.* [2004] and *Park* [2014]. The critical mixing fraction of the buoyancy sorting framework is also used by *De Rooy and Siebesma* [2008] to calculate the detrainment. *Gregory* [2001] use buoyancy in their entrainment formulation in combination with vertical velocity. A simpler approach is taken by *Lin* [1999] (also used in *Jensen and Genio* [2006]), where $\varepsilon = \lambda B^{\alpha}$, with the constants λ and $\alpha = -1.27$, and B the buoyancy.

Romps and Kuang [2010] found that a stochastic parameterization of entrainment, in contrast to a constant entrainment rate, is able to represent the observed variability between updrafts. This variability depends mostly on the variable entrainment rate during the ascent and much less on the conditions at cloud base. For their eddy-diffusivity/mass flux model, *Sušelj et al.* [2013] also use the stochastic approach, but with a constant entrainment rate below the level of condensation.

This study uses a variety of entrainment models, comparing them all in the same setup. Entrainment formulations with dependencies on height, buoyancy, vertical velocity, and stochastics are compared to a constant entrainment rate. This choice gives a broad spectrum of different concepts. Details about the entrainment formulations are described in section 3.

3. Method

We study parcel behavior by looking at a rising, entraining parcel model, with the set of equations coded as a standalone program. The parcel model is fed with vertical profiles diagnosed from the 3-D field of the LES. Different entrainment closures are applied and the results are intercompared.

3.1. Parcel Model Formulation

A parcel is defined here to represent an infinitesimally small particle, much smaller than the coherent structures of the turbulent field in which it rises. We assume that the parcel's life time is much shorter than the advective tendency of the bulk boundary layer, which motivates assuming steady state. The associated parcel model equations therefore describe the net change of the properties of such a small particle as it rises through the turbulent field. As the particle is infinitesimally small, carrying no mass, its area fraction is not considered. This approach is not unprecedented [e.g., *Neggers et al*., 2002; *Romps and Kuang*, 2010]. In addition, we assume that the parcel model also holds for small scales.

Accounting for these assumptions, the parcel model based on SW69 can be written as [*Siebesma et al*., 2007; *Neggers et al*., 2009]

$$\frac{\partial \Phi_u}{\partial z} = -\epsilon_u(\Phi_u - \Phi_e), \tag{1}$$

$$\overbrace{\frac{1}{2}(1-2\mu)\frac{\partial w_u^2}{\partial z}}^{acc} = \overbrace{-b\epsilon_u(w_u^2 - w_e^2)}^{mix} + B_u, \tag{2}$$

$$B_u = \frac{g}{\Theta_v}(\Theta_{v,u} - \Theta_{v,e}), \tag{3}$$

with Φ a conserved thermodynamic variable for moist adiabatic ascent (total specific humidity q_t or liquid water potential temperature Θ_l), ϵ_u the effective mixing rate, μ=0.15 and $b = 0.5$ proportionality constants for drag [e.g., *Romps and Charn*, 2015] and mixing, B the buoyancy, g the gravitational acceleration, Θ_v the virtual potential temperature, and $\bar{\Phi}$ the mean over the whole domain. "Acc" stands for the effective acceleration term, which includes the pressure homogenization, and "mix" denotes the mixing term. While we are aware that there are different values of μ and b used in the literature, *De Roode et al*. [2012] found that though our values might not be optimal for the RICO case, a range of values for μ and b will only result in small errors.

At this point we make some additional assumptions. The first concerns the source of entrained air, which is assumed to originate locally, adjacent to the parcel. This can be interpreted as an indirect way of introducing interactions with other parcels into the model. The properties of such parcels can differ greatly from the passive, cloud-free environment, for example when the adjacent air (or parcel) also sits inside a cumulus cloud. This sets this model apart from most previous multiparcel models, in which the parcels only interact with the passive environment. In practice, to achieve this interaction, the profiles of all grid columns as sampled from a fine-scale cumulus resolving model (LES) are given to the off-line rising parcel model. This should reveal how a rising parcel can react to different local environments. During its ascent the parcel is continuously diluted with air from the instantaneous LES column inside which it is rising; in (1)–(3) subscript "*e*" is replaced by "*Lc*" (LES-column) to reflect this lateral mixing model involving locally entrained air.

By using *Lc* in equation (3), B_u becomes a local buoyancy, describing the excess over the local environment. This is very different from a mean buoyancy which describes the buoyancy over the horizontal mean. The key difference is that parcels experience the local environment also in the buoyancy. It is to be expected that parcels sitting inside a buoyant LES cloud (i.e., mean buoyant) will not have a large local buoyancy.

The second assumption is that the parcels rise only vertically, not laterally. Alternatively, one could choose to use LES trajectories of rising parcels instead, which perhaps would better follow rising cumulus clouds during their life cycle. However, this approach is also not without problems. For example, model parcels which mix differently compared to the actual rising parcel will start to deviate from this trajectory. We therefore consciously adopt a simpler approach, by only considering purely vertical columns. While this simplifies the analysis, it still confronts the parcel model with many different environments; this should be sufficient for studying the potential impact of heterogeneous air on the fate of the parcel, and give insight into mechanisms like parcel screening and buoyancy sorting. The use of many different, but representative profiles allows a statistical assessment of parcel behavior.

The rising parcel model is thus vertically integrated with the environmental properties obtained from sampled columns from instantaneous 3-D LES fields. With this setup, we follow three aims:

1. To confront the classic rising parcel model with a heterogeneous environment, representative of a shallow cumulus cloud field.
2. To investigate the occurrence of parcel screening and buoyancy sorting mechanisms.
3. To explore the additional impact of the entrainment formulation.

This study exclusively focuses on gaining more insight into parcel model behavior in situations in which it might encounter different local environments. The use of a heterogeneous environment, which can be interpreted as introducing interactions between parcels, has not been a feature in most previous parcel models. In the mixing term, two factors can a priori be distinguished that can play different roles concerning the ascent of the parcels. The first factor, the local environment, has varying effects. Inside an LES cloud, where the difference between the parcel and the LES column can be small, the dilution is small, minimizing deceleration due to mixing. On the other hand, when a parcel leaves the LES clouds, the mixing can decelerate the parcel. The second factor, the entrainment, is given by the closure of the model. Beforehand it is not clear which factor will dominate. Therefore, to understand the behavior of the parcels we will investigate which factor dominates and has the larger effect on the ascent of the parcels.

3.2. Experimental Setup

For this study the SW69 rising parcel model is provided with vertical profiles as sampled from the LES model UCLALES [*Stevens et al*., 2005]. The LES-columns are sampled from the instantaneous 3-D fields of temperature, humidity, and vertical velocity, which are then used as the environmental variables appearing in equations (1–3). We stress that the parcel calculation does not affect the LES in any way.

For testing the SW69 rising parcel model the Rain In shallow Cumulus over the Ocean (RICO) case was chosen [*Rauber et al*., 2007], as it represents a clean undisturbed case of marine shallow cumulus. The campaign took place from November 2004 to January 2005 near Antigua and Barbuda in the Atlantic Ocean in the trade wind region. Measurements were conducted by three aircrafts, one research ship and land stations. LES simulations based on this case have been intercompared and confronted with measurements [*van Zanten et al*., 2011], showing that LES models do well in reproducing its key features.

After 9 h the spin-up time of the simulation has passed. The time period selected for analysis in this study therefore starts at 9 h and ends at 12 h, which gives enough data for analysis without being computationally very costly. During these 3 h, every 200 s the LES profiles of all columns are given to the parcel model. The simulated model domain is 14 km × 14 km × 4 km with a resolution of 100 m in the horizontal and 40 m in the vertical, which is the same resolution as used by *van Zanten et al*. [2011]. The UCLALES model we use has a Smagorinsky type subgrid scheme and was part of the intercomparison in *van Zanten et al*. [2011].

The rising parcels are initialized at the lowest model layer with

$$\Phi_u(x,y) = \overbrace{\bar{\Phi}_{Lc}(x,y)}^{environment} + \overbrace{\Delta\Phi}^{surface\ \ perturbation}, \tag{4}$$

$\Delta\Phi$ the surface perturbation, and $\bar{\Phi}$ the mean over the grid cell. This formulation gives all parcels an initial excess of Φ and thereby ensures that all parcels reach the cloud layer. The parcel initialization height is assumed to be situated inside the surface layer, so that a constant flux with height can be used, which means that the perturbation can be written as

$$\Delta\Phi = c\,\overline{w'\phi'_{sfc}}/\sigma_w, \tag{5}$$

as proposed by *Troen and Mahrt* [1986], where σ_w is calculated using the relation proposed by *Holtslag and Moeng* [1991] and c is a scaling factor. We choose to keep c constant for simplicity to be able to assess only the variability of the environment. This procedure is fully described in the ECMWF IFS documentation, Part 4, Chapter 3. This initialization procedure is also used in *Neggers et al*. [2009]. Condensation within the parcel follows the common method used in *Sommeria and Deardorff* [1977].

3.3. Implementation Details

Next, the details of the implementation of the entrainment models as listed in Table 2 are briefly discussed:

1. The first, simplest possible entrainment model assumes the entrainment to be a constant c for all parcels.

Table 2. Root-Mean Square Error of the Best Fit for Various Entrainment Models

Entrainment Model	Parameter	Best Fit	RMSE
Constant	c	1/70	0.0112
1/w	τ	100	0.0099
1/z	c	50	0.0112
1/B	λ	1.2×10^{-6}	0.0095
Stochastic	c	1/25	0.0096

2. For the dependency on height, the model by *Siebesma et al.* [2003] is used, where $\varepsilon = c\,(1/z)$ and c is a constant to be calibrated.
3. The model by *Lin* [1999] is used for the buoyancy dependency, where $\varepsilon_i = \lambda B_{i-1}^{\chi}$. Here i denotes the level where the entrainment is calculated. Since we need the entrainment to calculate the buoyancy of the current level, the buoyancy of the previous level is used. We choose $\alpha = -1.27$, which *Lin* [1999] found to be a good constant value for α and which we found to be suitable for this study as well. The constant to be calibrated here is λ. We use the buoyancy from the LES model, i.e., the local environment, to calculate the entrainment only if the buoyancy is positive. In previous studies [e.g., *Jensen and Genio*, 2006], the parcel stops at the level of neutral buoyancy. To ensure that the parcels in our study do not continue to rise with a negative buoyancy, we set the entrainment rate for negative buoyancies to a high value of 0.1. This value is arbitrary, but the results are not sensitive to this value so we assume it to be reasonable.
4. For the vertical velocity dependency the model by *Neggers et al.* [2002] is used: $\varepsilon = \eta/(\tau w)$, with w the vertical velocity of the parcel, η a calibration factor, which in this study is set to one, and τ the turnover time scale, which is to be determined.
5. To include a stochastic model, we developed a very simple model inspired by *Romps and Kuang* [2010]. We implemented the model in a way that gives the highest variability, since the increased variability is the main characteristic of this model compared to the other models. Therefore, we calculated the entrainment rate for each parcel only once at the beginning: $\varepsilon = c\ r$. c is the constant to be calibrated and r is a random number picked from a gamma distribution $f = \frac{y^{\alpha-1}e^{-y/\theta}}{\theta^{\alpha}\Gamma(\alpha)}$ after *Marsaglia and Tsang* [2000], where the normal distribution needed for the calculation of the gamma distribution is calculated with the Marsaglia polar method [*Marsaglia and Bray*, 1964]. For the gamma distribution, two parameters need to be specified, the shape parameter α and the scale parameter θ. For the highest variability in entrainment we chose $\alpha = 2$ and $\theta = 0.5$, which puts the average of the function at 1 and thus makes the calibrated parameter c comparable to the constant entrainment rate.

Since the main goal is to evaluate the dependency of parcel state on a range of different variables, simple formulations are used to facilitate the interpretation. The main constant in each formulation is calibrated so that the vertical profile of the number of parcels still rising best matches the cloud fraction profile in the LES (described in detail in the next section). This means that here it is implicitly assumed that all cloudiness in the RICO case is associated with rising parcels. Although this assumption is certainly simplistic, the main aim here is to capture the typical vertical structure of the number of rising parcels in the cloud layer. We chose the minimum RMSE to calibrate the entrainment models instead of using the constants from the literature because (i) the constants in the literature are often determined for whole cloud populations, not single parcels, resulting in a conceptual mismatch; (ii) in the literature different cases are used to calibrate the models, whereas we study the RICO case for all models, independent of the cases for which the models were designed; and (iii) each entrainment model should be given a chance to perform at its best. The details of this calibration are described in the next section. It should be noted that our main goal is to document parcel behavior, and its dependence on the environment as well as on the entrainment model. The detailed discussion of each entrainment model itself, as well as its possible applicability, is not in the scope of this study; for this we refer to the individual publications that describe each model (see section 2).

4. Results

4.1. Cloud Fraction

The "cloud area fraction" for (i) the LES, $a_c^{LES}(z)$ and (ii) for the parcels, $a_c^{parcels}(z)$, is defined as

$$a_c^{LES}(z) = \frac{1}{N_x N_y}\sum_{i=1}^{N_x}\sum_{j=1}^{N_y} I^{LES}(i,j),$$

$$a_c^{parcels}(z) = \frac{1}{N_x N_y}\sum_{i=1}^{N_x}\sum_{j=1}^{N_y} I^{parcels}(i,j),$$

respectively, with I an indicator function defined as

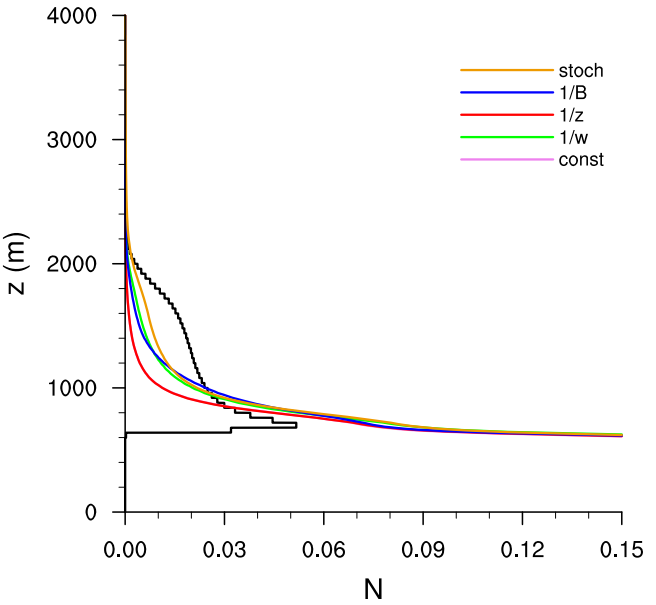

Figure 2. Profiles of cloud fraction for the simulations with entrainment models depending on a constant, on vertical velocity, on height, on buoyancy, and on stochastics, and profile of the LES cloud fraction. The normalized number of cloudy grid boxes of the LES for each level (solid black line) and the normalized number of rising parcels inside columns with an LES cloud for the five different models (colored lines) are shown, averaged over the analysis time.

$$I^{LES}(i,j)=\begin{cases}0 \text{ for } q_l=0\\ 1 \text{ for } q_l>0\end{cases},$$

$$I^{parcels}(i,j)=\begin{cases}0 \text{ for } z>z_t(i,j)\\ 1 \text{ for } z\le z_t(i,j)\end{cases},$$

with z_t the termination height of the parcel. The cloud area fraction defined here describes the fraction of those grid boxes containing parcels, which have a negligible size inside the grid box (see section 3.1). As argued above, the fractions $a_c^{LES}(z)$ and $a_c^{parcels}(z)$ are for simplicity considered to be comparable, because the parcels condense above cloud base and resemble the cumulus clouds in RICO, where most clouds are convective and surface-driven.

Figure 2 shows the ability of the entrainment models to reproduce the cloud fraction profile of the LES. In the LES the lifting condensation level (LCL) is between 600 and 700 m. Above the LCL there is a maximum in cloud fraction, with a decrease with height and the highest clouds reaching about 2200 m. Similar profiles of the cloud fraction were found by *van Zanten et al*. [2011] and *Siebesma and Cuijpers* [1995].

Differences exist between $a_c^{LES}(z)$ and $a_c^{parcels}(z)$ throughout the subcloud layer, since the parcels start to rise at the surface and the fraction is constant in the subcloud layer for all entrainment models. The heights of cloud base and cloud top are mostly well captured, but all entrainment models overestimate the cloud fraction near cloud base and underestimate it higher up. However, though there are differences in the ability of the models to represent the vertical structure, all models are able to reproduce the cloud fraction to some degree.

To quantify the capability of the entrainment models to capture the vertical structure, the following root mean square error is calculated:

$$RMSE=\sqrt{\frac{1}{Z}\sum_{z=1}^{Z}(N_u(z)-N_{Lc}(z))^2}, \tag{6}$$

with Z the number of horizontal levels that are taken into account and N_u and N_{Lc} the number of updrafts and cloudy grid boxes at each level, respectively. The vertical range in which this evaluation takes place is defined by the maximum cloud fraction of the LES as the lower boundary, and the top of the LES cloud fraction as the upper boundary.

Using this RMSE, a parameter optimization was performed by varying the constant parameters of the entrainment formulations and comparing the cloud fraction of the parcels to the LES cloud fraction. The RMSE for the different entrainment models are displayed in Figure 3. From this analysis, the parameter giving the smallest RMSE was chosen for each entrainment model. Though there is some variation among the vertical profiles produced by the various entrainment models, which is reflected by the RMSE, it is relatively small since all entrainment models yield the same basic decreasing cloud fraction with height. A summary of the optimized parameters is given in Table 2. These parameters differ slightly from the parameters in the literature. For the vertical velocity dependency, τ is smaller than proposed by *Neggers et al*. [2002] based on an analysis of whole clouds; in our application a lower τ is required to make parcels stop at cloud base. For

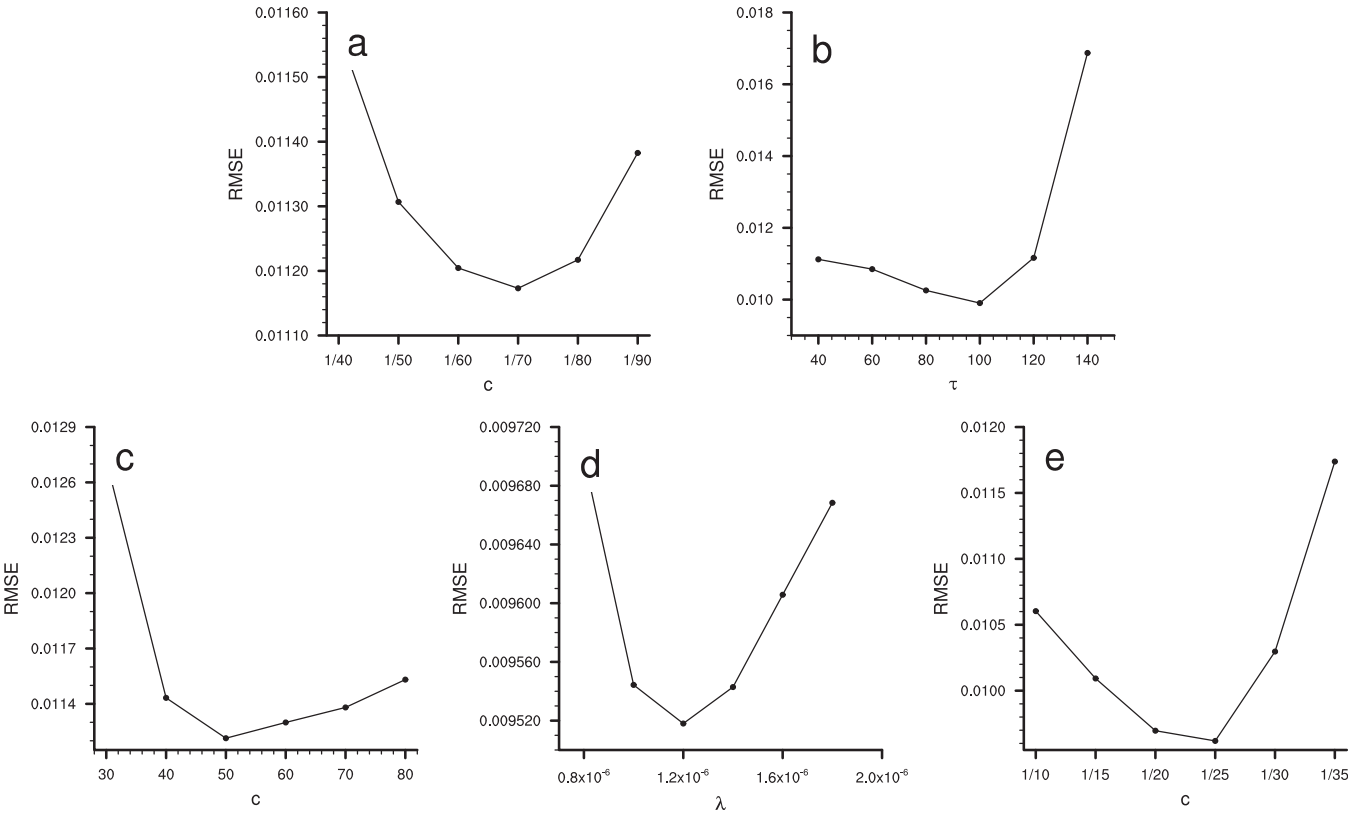

Figure 3. RMSE for varying parameters of entrainment models which depend (a) on a constant, (b) on vertical velocity, (c) on height, (d) on buoyancy, and (e) on stochastics.

the same reason, the value for c in the height dependent formulation as well as λ in the buoyancy dependency and c in the constant formulation are slightly larger than the values in the literature. Our stochastic formulation deviates too much from the original formulation by *Romps and Kuang* [2010] to allow a direct comparison.

By finding the most suitable parameter, we prepared the entrainment models such that each model is calibrated to this specific application and case. Since the main goal of our study is to investigate the behavior of the parcels, we limit the number of different parameters tested, which is nevertheless detailed enough for a comparison of the different entrainment models.

Beside cloud fraction, another way to compare the entrainment models is by looking at the variability among parcels for each model. To this purpose we calculated the variance among the rising parcels

$$\sigma^2_{q_t} = \frac{\sum_{q_t} \left(q_{t,u}(z) - \overline{q_t}(z)\right)^2}{n(z)}, \tag{7}$$

with n the number of rising parcels present at height z, $q_{t,u}$ the total specific humidity of the parcel, and $\overline{q_t}$ the average over all rising parcels. Thus, for each level we only take into account those parcels that are still rising. The behavior of the parcels is influenced by both q_t and Θ_l. In the following we will only show the results for q_t for brevity.

In Figure 4 the humidity variance is used to compare the different entrainment models. All entrainment models show the same order of magnitude for the variance. The entrainment model depending on the buoyancy exhibits one of the larger spread among the parcels. We hypothesize that the underlying mechanism of this behavior is the buoyancy sorting concept [*Kain and Fritsch*, 1990]. When a group of parcels rises inside an LES cloud, the LES buoyancy is large, implying weak dilution of the rising parcels when using this entrainment model. However, as soon as a parcel leaves the cloud, the LES buoyancy B_{Lc} becomes small, so that the parcel starts to dilute more efficiently. Parcels thus become very sensitive to their environment,

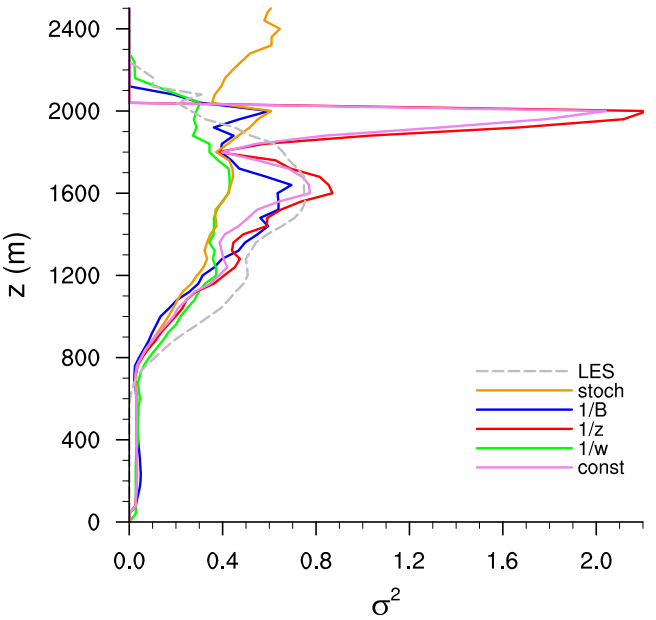

Figure 4. q_t-variance for the five entrainment models for all rising parcels with the LES variance as a reference.

with the buoyancy-based entrainment model amplifying the impact of the environment that we already see with the constant entrainment model. The peak in the variance near cloud top for the formulations depending on a constant and height are due to a small number of still rising parcels.

It is interesting to note that the variance of the stochastic approach and the constant entrainment have similar magnitudes. More insight into the buildup of the variance among parcels is provided by Figure 5, showing the difference in variance between a subset of parcels, of which the termination height is equal to or higher than 1800 m, and all rising parcels. Here 1800 m is chosen as a height defining high reaching parcels. For the subset of high-reaching parcels the variance at lower levels is smaller; this holds for all entrainment models. This suggests that the properties of high reaching parcels are more similar during their ascent compared to the full ensemble. Apparently, these parcels are screened off from the hostile cloud-free environment by the local environment which supports the ascent. This result further confirms that the local environment has a strong influence on the rising parcels. Especially the variance of the entrainment models depending on buoyancy and vertical velocity is smaller for the high-reaching subset. The vertical velocity dependency exhibits a positive feedback since increasing vertical velocity decreases the mixing rate which in turn supports an increasing vertical velocity. A higher buoyancy stimulates an increased vertical velocity, resulting in a similar behavior of those two entrainment models.

4.2. Differences Among Parcels

To better understand the differences between rising parcels we now segregate the behavior of parcels as a function of their termination heights. In this and the following analyses we only consider the simplest entrainment model with a constant entrainment rate. The argumentation for this is that it highlights the role of the environment; the secondary dependence on the entrainment model as reported earlier also justifies this choice.

Figure 6 shows the median q_t-profile of all parcels, as well as the spread among them. When categorized into different termination heights with bins of 200 m (Figure 7), several differences become apparent. With increasing termination height, the interquartile range increases slightly, probably because more variable local environments are encountered. Also, the high reaching parcels are more successful in maintaining their humidity. Apparently, parcels with a high humidity are more successful in rising far. For the two highest bins, this difference is not present at all heights due to the relatively small number of high-reaching parcels. The humidity is mainly influenced by the local environment, which again illustrates the importance of the local environment on the behavior of the rising parcels. At lower levels below cloud base, all bins have a similar humidity (Figure 8a) because all parcels were initialized the same. The difference between the parcels is caused by the different environments they encounter.

From this analysis, the effective mixing for each bin can be quantified by using equation (1) to yield

$$\epsilon^b_{bin} = -\frac{\frac{\partial}{\partial z}\langle q_{t,u}\rangle^b}{\langle q_{t,u}\rangle^b - \overline{q_t}} = \frac{\langle \epsilon_u \left(q_{t,u} - q_{t,Lc}\right)\rangle^b}{\langle q_{t,u}\rangle^b - \overline{q_t}} \tag{8}$$

and discretized

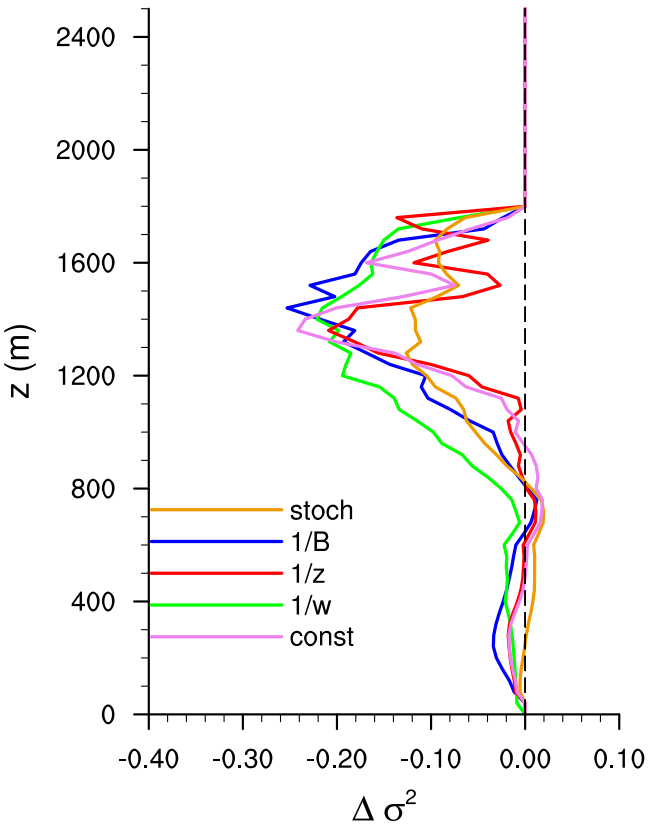

Figure 5. Difference between the q_t-variance of parcels reaching at least 1800 m and all rising parcels for the five entrainment models.

$$\epsilon^b_{bin} \approx -\frac{\frac{q_{t,u}(z_2)-q_{t,u}(z_1)}{z_2-z_1}}{q_{t,u}(z_1)-\overline{q_t}(z_1)}, \qquad (9)$$

where $\langle\rangle^b$ indicates the mean over all parcels in bin b, and $\overline{(..)}$ indicates the horizontal mean over the whole domain. Note that ϵ^b_{bin} is conceptually different from the entrainment rate for individual parcels ϵ_u: the former represents the entrainment rate needed to reproduce the mean of the bin with a bulk parcel model that acts on the horizontal mean $\overline{q_t}$. We adopt this definition to allow comparison of our results with previous studies of bulk entrainment.

To calculate the entrainment with equation (9) we used $z_1 = 800$ m and $z_2 = 1360$ m as upper and lower heights for all bins. The upper level was chosen because it is the top of the parcels from the lowest bin. The results were found not to be sensitive to this choice (not shown). The resulting entrainment rates for all bins are compared in Figure 8b. The bin of the fortunate, highest rising parcels has a low entrainment rate, enabling them to rise far, while the bin with the unfortunate parcels has a high entrainment rate. The range of entrainment rates lies between 0.0015 and 0.003 m^{-1}. In the literature, similar values were found for bulk population statistics [*Siebesma and Cuijpers*, 1995].

4.3. Case Studies

To gain more insight into the relation between parcel and local environment, two individual parcels with very different properties are selected as opposing case studies. Parcel state variables and budget terms will be investigated, focusing on the differences between these two parcels. This should provide insight into what causes the net behavior of a parcel in general, and its response to its direct environment.

4.3.1. The Fortunate Parcel

The first case is a parcel with one of the highest maximum vertical velocities, which falls in the bin of the highest reaching parcels as discussed in the previous section. This column is interpreted as an example of a strong updraft with a high vertical velocity and a high termination height, rising in the most favorable environment and therefore called "fortunate parcel." These strong parcels are relatively rare [*Plank*, 1969] but are illustrative to study. The LES cloud in which this updraft is embedded is shown in Figure 9a. The profiles of vertical velocity and q_t-excess of the parcel over the environment as well as the profiles of the buoyancy and $w'q'_t$ (solid lines) are shown in Figure 10. The high termination height of this parcel is associated with a high vertical velocity, increasing until about 2000 m. Up to that height, the q_t-excess is small, being first slightly positive and above 1600 m becoming slightly negative, indicating a small q_t difference between the parcel and its direct environment. This behavior is caused by the presence of an LES cloud in the column, associated with a relatively high $q_{t,Lc}$. The buoyancy B_u is slightly positive for most of the ascent of the parcel. Near its termination height the parcel vertical velocity decreases rapidly while the q_t-excess increases rapidly. This probably reflects the parcel overshooting out of the LES cloud. At the top of the LES cloud the $q_{t,Lc}$ decreases abruptly (not shown), causing the difference between the parcel and its environment to increase. Near the termination height the negative B_u contributes to the stopping of the parcel.

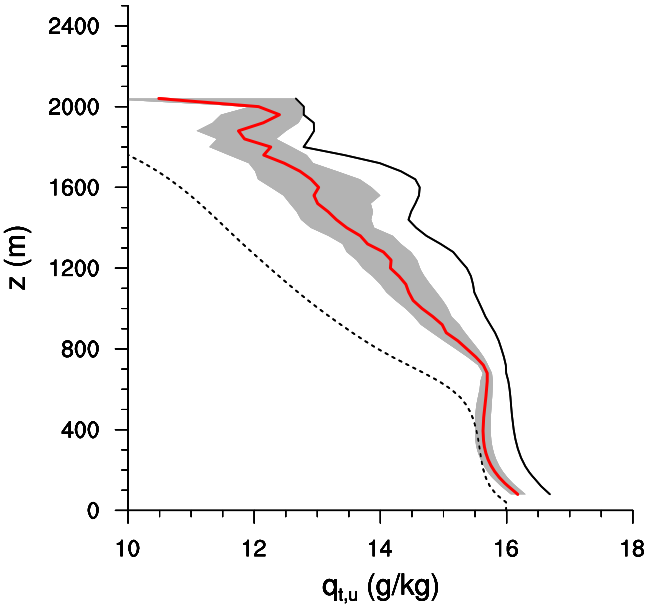

Figure 6. Median of q_t for all rising parcels (red), interquartile range (gray), maximum q_t for each level (solid black) and mean q_t of the local environment (dashed black).

The product $w'q_t'$ is shown in Figure 10d, expressing the impact on vertical transport. The profile closely resembles that of the q_t-excess, with a very small positive value until a height of about 1600 m and a slightly negative value between 1600 and 2000 m. (Note that this product represents the hypothetical transport relative to the *direct* environment; the parcel is "sailing" on top of an LES cloud. Accordingly, a negative local value could still be associated with a positive value with respect to the horizontal mean). Near the termination height this term peaks due to the combined high values of vertical velocity and q_t-excess at that height.

The results illustrate that the parcel reacts immediately to changes in its environment. As long as the vertical velocity inside the LES cloud is positive, the parcel follows with a similar

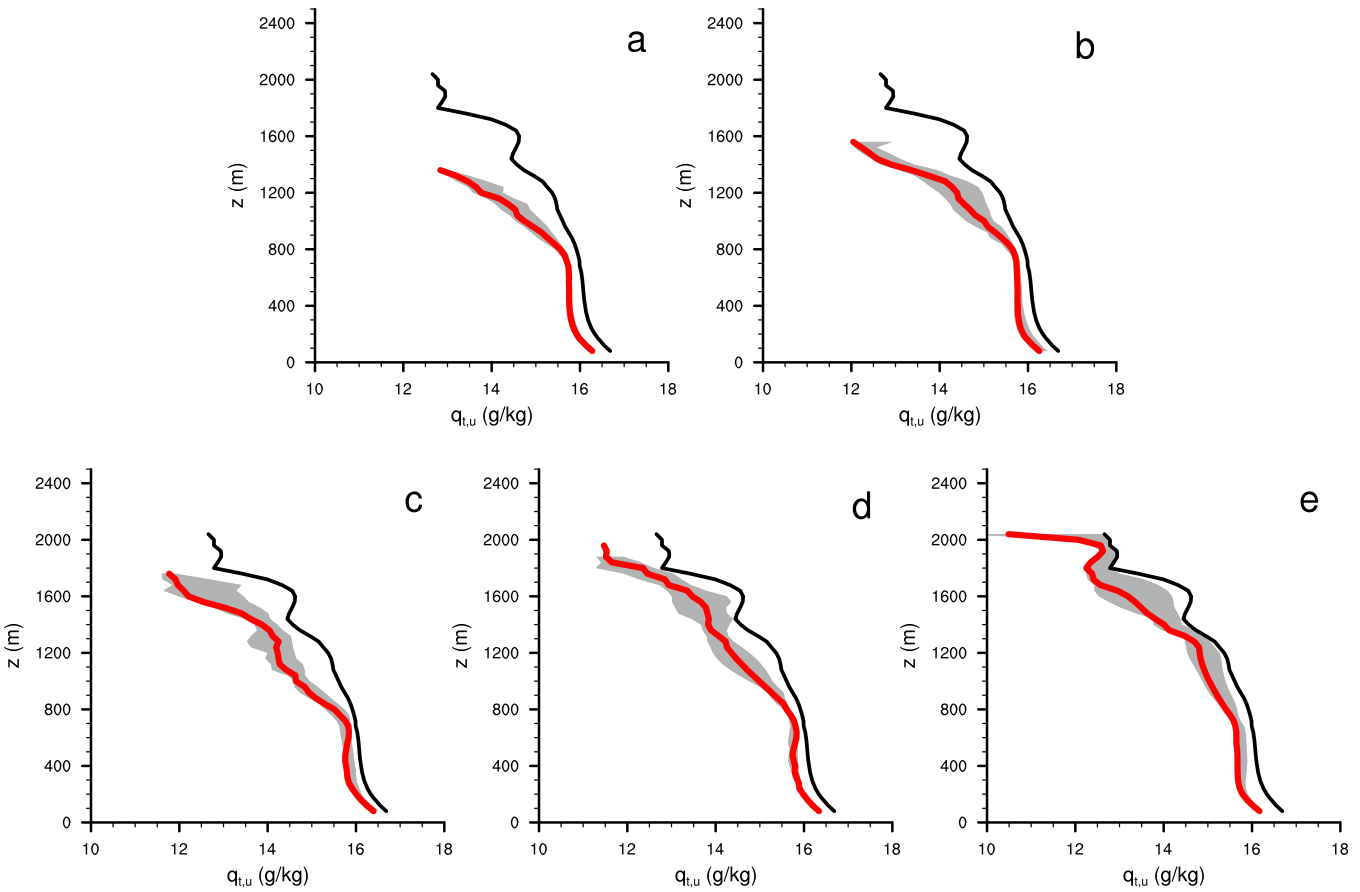

Figure 7. Median of q_t for all rising parcels (red), interquartile range (gray), maximum q_t for each level (solid black) for all rising parcels that reach between (a) 1200 and 1400 m, (b) 1400 and 1600 m, (c) 1600 and 1800 m, (d) 1800 and 2000 m, and (e) 2000 and 2200 m.

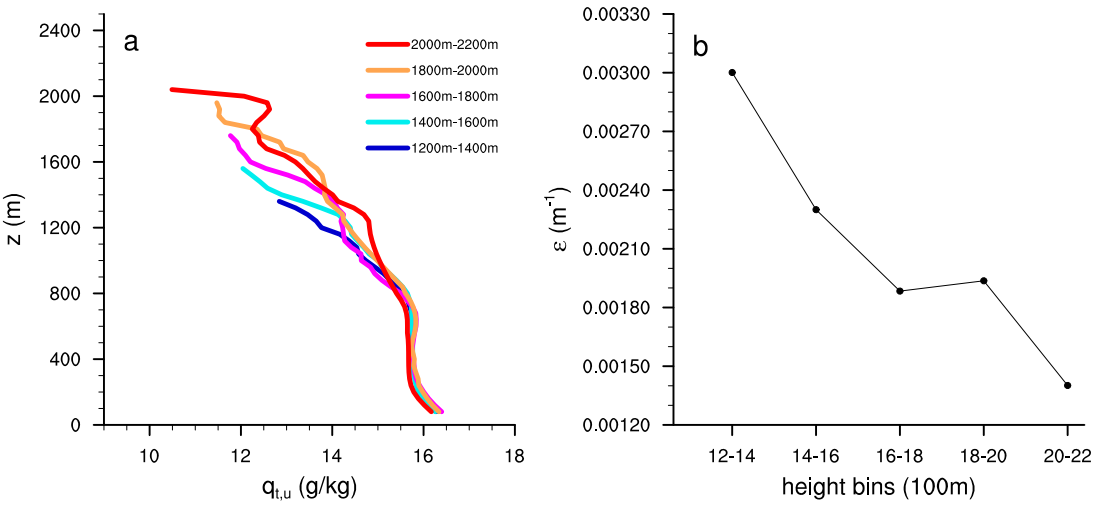

Figure 8. Median of (a) q_t and (b) bulk entrainment rate for different height bins for the model with constant entrainment.

vertical velocity; the picture emerges that it is sailing along with the cloud, profiting from its protected status. Once the parcel shoots out of the cloud, it quickly reaches its termination height. The vertical extent of this overshooting layer is small, suggesting that parcels cannot live long outside an LES cloud.

4.3.2. A Less Fortunate Parcel

wAnother parcel is studied as an opposite example. This parcel, taken from the second highest category of section 4.2, does not reach that high, and could therefore be labeled as a "less fortunate" parcel. It is a less extreme case than the "fortunate parcel" and serves as an example of the variety of parcels' fates. Figure 10 shows the profiles of this less fortunate parcel. The q_t-excess differs substantially from the fortunate parcel in its second peak between 1200 and 1600 m, which corresponds to a decrease in its vertical velocity w_u. Somewhat counterintuitively, its buoyancy B_u at this height is mostly positive and much larger than the buoyancy of the fortunate parcel. The profile of $w'q_t'$ resembles the profile of the q_t-excess. Figure 9b shows the LES environment in which the less fortunate parcel rises. It contains two clouds, and although the parcel rises at the edge of the higher cloud, this still results in a double peak in the liquid water mixing ratio at about 1400 and 1800 m. Because between those two peaks, $q_{t,Lc}$ is at a minimum, $q_{t,u}$ is now larger than $q_{t,Lc}$, associated with a peak in the q_t-excess. This behavior, featuring a gap in the LES cloud, can in this framework be loosely interpreted as a particle being detrained by one cloud and subsequently being entrained by another.

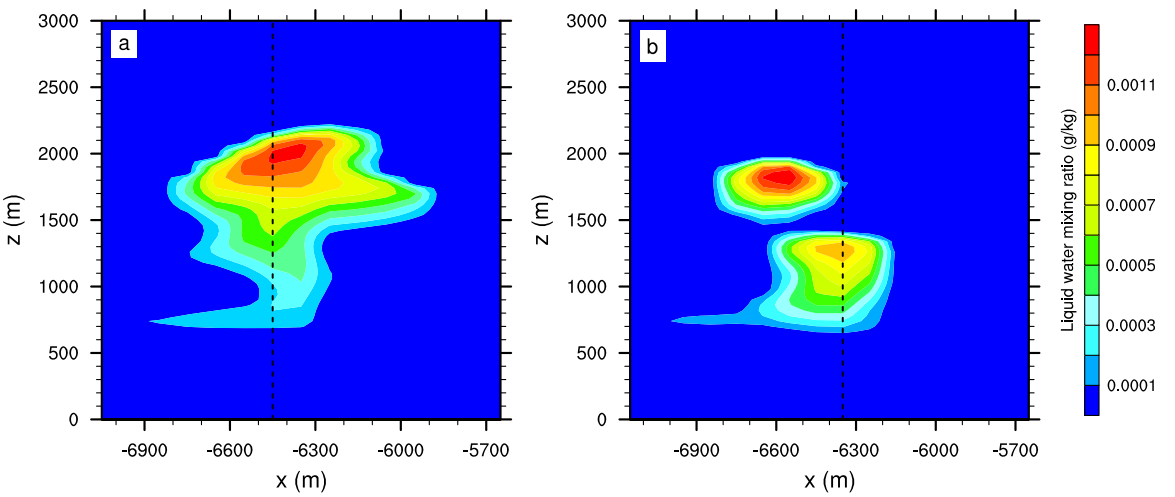

Figure 9. Part of a vertical cross section of the liquid water mixing ratio of the LES around (a) the fortunate parcel and (b) the less fortunate parcel (dashed line is the location of the studied columns shown in Figure 10).

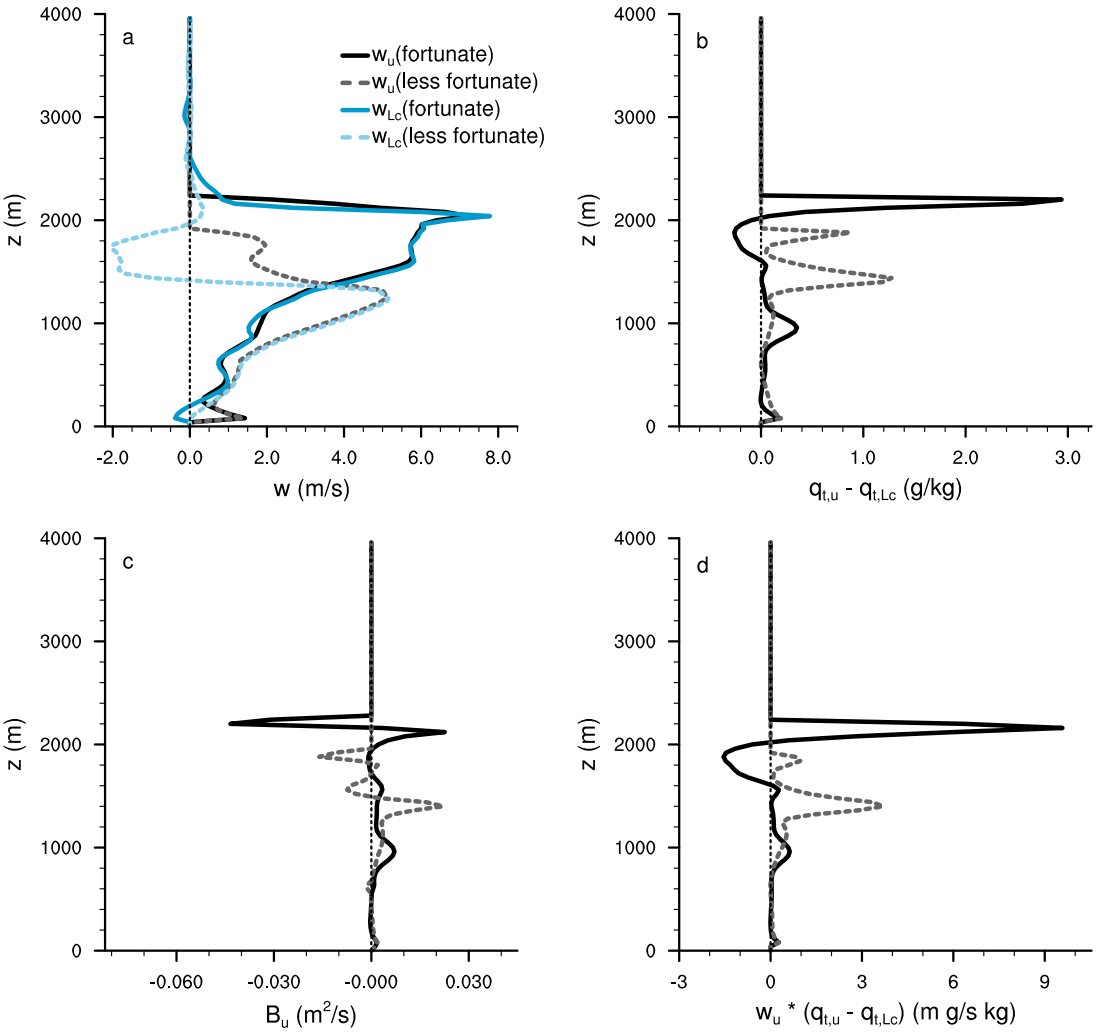

Figure 10. Profiles of (a) vertical velocity, (b) q_t-excess, (c) buoyancy, and (d) $w'q_t'$ for the fortunate (solid line) and the less fortunate parcel (dashed line) and the LES columns (blue).

The parcel behavior for this less fortunate parcel further highlights how strongly the parcel reacts to its direct environment. Only when it leaves a cloud is it actively able to do transport relative to its direct environment; however, the hostile air then quickly and efficiently reduces both its kinetic energy and excess properties.

4.4. Budget Analyses

4.4.1. Fortunate Parcel

The behavior of the rising parcels can be revealed in more detail by studying the different terms of the budgets that control the behavior of the parcels. Two terms in the parcel's kinetic energy budget can have opposing effects, the mixing term and the buoyancy B_u (equation (3)). Figure 11a shows the variables making up the buoyancy B_u for the fortunate parcel, including the virtual potential temperature of this parcel $\Theta_{v,u}$, the LES column $\Theta_{v,Lc}$, and the average over the whole domain $\overline{\Theta_v}$. B_u and $B_{Lc}=g(\Theta_{v,Lc}-\overline{\Theta_v})/\overline{\Theta_v}$, are also shown for reference. The $\overline{\Theta_v}$ profile shows the well mixed subcloud layer with a more or less constant value, a conditionally unstable lapse rate in the cloud layer and an inversion at about 1900 m. In the cloud layer $\Theta_{v,Lc} > \overline{\Theta_v}$, which is in accordance with the rising of the convective cloud in the column. Near the top of the cloud $\Theta_{v,Lc}$ is smaller than $\overline{\Theta_v}$. Compared to $\Theta_{v,Lc}$, $\Theta_{v,u}$ is only marginally larger, but extends slightly higher. B_{Lc} is positive up to the height where $\Theta_{v,Lc}$ gets lower than $\overline{\Theta_v}$. Here B_{Lc} becomes negative up to the cloud top. In contrast, the updraft buoyancy B_u is only marginally positive. At the height where the LES cloud reaches its top, B_u has a positive peak, until $\Theta_{v,u}$ sharply decreases as the particle overshoots the

cloud. These profiles show that the parcel model feels its local environment and reacts to it; it sails with the LES cloud in a weakly buoyant state.

The analysis of the kinetic energy budget (equation (2)), including the buoyancy term, the acceleration term, and the mixing term, is shown in Figure 11c. Between cloud base and about 1800 m, the buoyancy and the mixing term are relatively small, and the acceleration mostly follows the mixing term. Above 1800 m, the mixing term dominates the budget up to shortly beneath cloud top. Note that the profile of the mixing term depends on $(w_u - w_{Lc})$ (see equation (2)). Between 1000 and 2000 m the term $w_u^2 - w_{Lc}^2 < 0$ (see Figure 10), causing the mixing term to become positive. The opposite is true between 2000 m and the termination height, resulting in a negative mixing term. At cloud top B_u takes over with a negative peak, while the mixing is already zero. Apparently, when the parcel shoots out of the cloud, its local buoyancy B_u becomes positive but is outdone by the suddenly strongly negative mixing term, causing the parcel to dilute and quickly loose its buoyancy. In other words, mixing is more important than buoyancy in the kinetic energy budget.

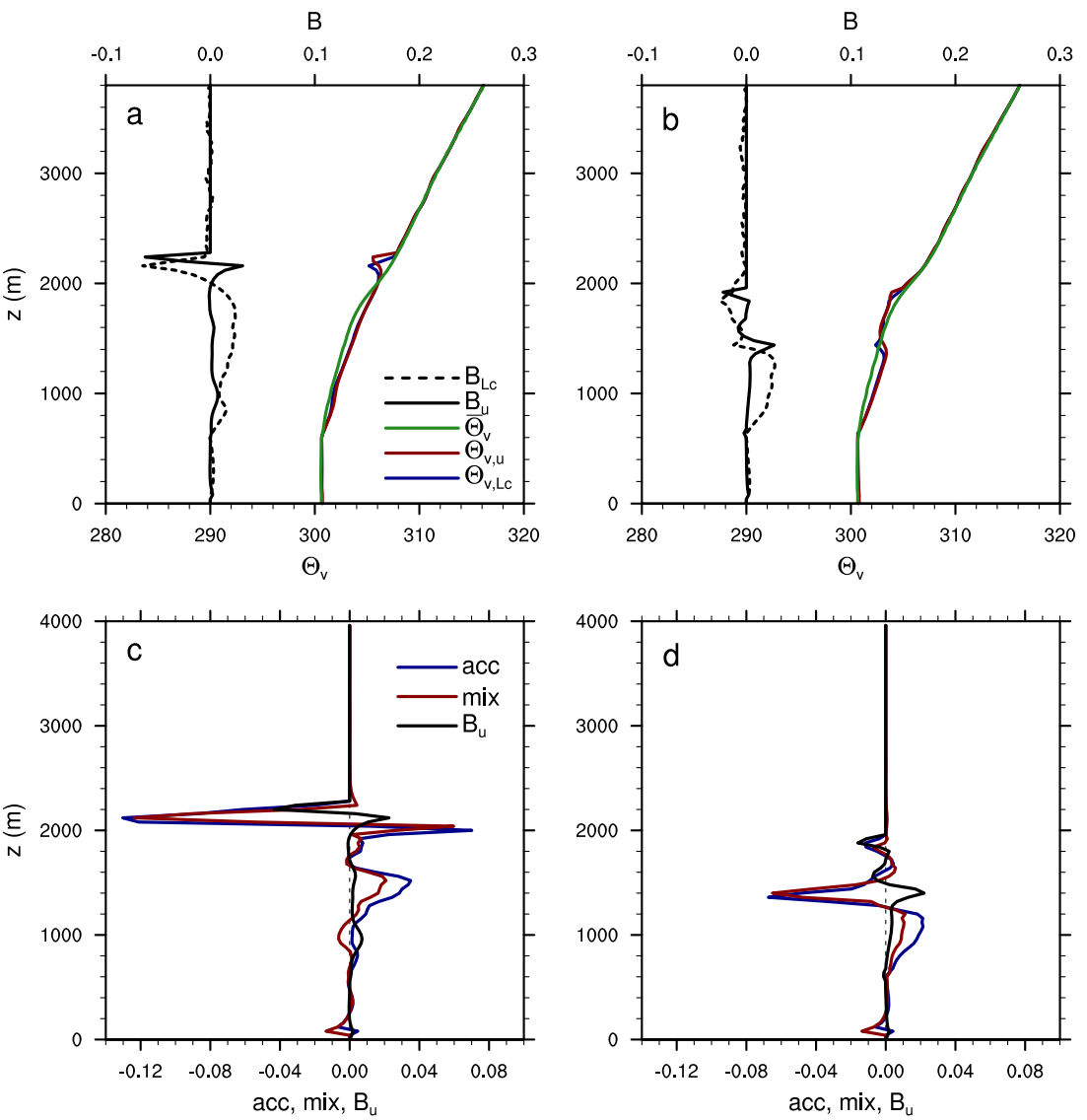

Figure 11. Buoyancy and contributing terms (equation (3)) for (a) the fortunate parcel and (b) the less fortunate parcel, and the budget analysis for the kinetic energy (equation (2)) for (c) the fortunate parcel and (d) the less fortunate parcel.

4.4.2. Less Fortunate Parcel

The budget analysis for the less fortunate parcel is shown in Figures 11b and 11d. Compared to Figure 11a, Figure 11b shows that $\Theta_{v,Lc}$ becomes smaller than $\overline{\Theta_v}$ at a lower height. There is an area around 1400 m where $\Theta_{v,u}$ is much larger than $\Theta_{v,Lc}$. In this area, B_{Lc} has a minimum, while B_u peaks. This area corresponds to the gap in the cloud (Figure 9b).

For the kinetic energy budget (equation (2) and Figure 11d), in the lower part of the cloud layer, the mixing term is positive while the buoyancy is small, resulting in a slightly positive acceleration term which enables the parcel to rise with the background LES cloud. Above about 1200 m, the mixing term becomes negative because $w_u - w_{Lc} > 0$ (see Figure 10). This mixing slows the parcel, causing the vertical velocity to decrease, because the mixing term has a higher magnitude than the suddenly positive buoyancy B_u. As the parcel enters the second LES cloud, it keeps decelerating, mainly because w_{Lc} is mostly negative (a passive cloud). As it overshoots the second cloud, negative buoyancy B_u efficiently slows the parcel down to a standstill.

At this point the following picture emerges about how parcels interact with a heterogeneous environment. Inside an LES cloud the local parcel buoyancy B_u is small, while its properties are close to that of the background; as a result, it is able to move with the cloud, being screened off from the hostile environment. As soon as it leaves the cloud, however, the mixing term starts to dominate the kinetic energy budget and ensures that the parcel quickly loses its excess properties, in the process becoming more important than the buoyancy. This mechanism effectively sorts out the parcels outside of clouds from the ones inside clouds. Given the dominance of the mixing term, this process could be referred to as a "mixing-sorting mechanism."

It is interesting to draw parallels with the buoyancy sorting mechanism as proposed by *Kain and Fritsch* [1990]. The main difference is that the buoyancy sorting mechanism is formulated in terms of the total buoyancy of a parcel over the mean state, $B_{Lc}+B_u$, while the mixing-sorting mechanism as described above is formulated in terms of the local B_u alone. In principle, they describe the same process, of parcels decelerating when leaving a cloud. However, as we find that the mixing term is in the end responsible for slowing down (and sorting out) the parcel, and not the buoyancy term, one could argue that mixing-sorting is a more appropriate name for this process.

5. Summary and Conclusions

In this study the potential impact of the local environment on the fate of a rising parcel is investigated. To this purpose a simplified setup was used, with parcels interacting with profiles that reflect the heterogeneous turbulent environment that they may encounter during their ascent. This way, interaction with other parcels is indirectly represented, which is a novelty in multiparcel modeling. In addition, the method is designed to enable the investigation of well-known mechanisms like parcel screening and buoyancy sorting. Different entrainment models were used in the same setup to investigate the effect of the entrainment parameterization on parcel behavior. An LES was used to generate a shallow cumulus cloud field, providing the range of different local environments that is required for this study.

We find that the most important factor determining the eventual parcel termination height is the local environment that it encounters on its way; the formulation of the entrainment model is of secondary importance. The entrainment model depending on the background buoyancy performs best. We speculate that the information of the state of the environment captured by the background buoyancy can explain this. The results further suggest that (i) parcel screening is efficient in boosting their termination height, (ii) parcels quickly lose their excess properties when leaving a protective in-cloud area, (iii) mixing dominates over local buoyancy in the kinetic energy budget of these parcels, and (iv) initial conditions seem to be less important that the mixing.

Despite the simplicity of our method, for example in the use of vertically sampled LES profiles to act as parcel environments and the omission of life cycle effects, the method is already successful in providing insight into some important mechanisms in shallow cumulus convection. This includes the parcel screening effect, the buoyancy sorting mechanism, and the importance of the local environment over the entrainment formulation. It would be interesting to explore if profiles obtained from LES trajectory analyses would yield the same results. This is considered a future research topic.

This study makes use of entrainment models that have been proposed in the literature. It is beyond the scope of this study to validate these models, or to derive new ones. The sole aim of including many different dependencies is to find out if any of these entrainment models can diminish the apparently dominant role of the local environment in determining parcel termination height. It is clear from the results that none can do so.

What do the results and insights obtained in this study imply for the parameterization of shallow cumulus convection? Perhaps the most important consequence is that the local environment encountered by rising parcels should be taken into account in the associated budget equations. This can be achieved either indirectly, by perhaps using a stochastic entrainment closure to mimic a chance encounter with heterogeneous air, or directly, by letting rising parcels in an ensemble somehow interact with each other. The development of such models is considered a future research opportunity. Perhaps the results obtained in this study can provide some guidance in this effort.

Acknowledgments
This project was funded by the Helmholtz Association in the framework of the Helmholtz Water Network and supported by the Graduate School of Geosciences of the University of Cologne. The simulations were run on CHEOPS, the cluster of the Regionales Rechenzentrum of the University of Cologne, and JURECA, Jülich Research on Exascale Cluster Architectures. The authors would like to thank Susanne Crewell and Vera Schemann for help in preparing the manuscript and two anonymous reviewers for their helpful suggestions. The LES data used in this study can be obtained from the corresponding author upon request.

References

Bretheron, C. S., J. R. McCaa, and H. Grenier (2004), A new parameterization for shallow cumulus convection and its application to marine subtropical cloud-topped boundary layers. Part I: Description and 1D results, *Mon. Weather Rev.*, *132*, 864–882, doi:10.1175/1520-0493(2004)132<0864:ANPFSC>2.0.CO;2.

Chikira, M., and M. Sugiyama (2010), Cumulus parameterization with state-dependent entrainment rate. Part I: Description and sensitivity to temperature and humidity profiles, *J. Atmos. Sci.*, *67*, 2171–2193, doi:10.1175/2010JAS3316.1.

Dawe, J. T., and P. H. Austin (2013), Direct entrainment and detrainment rate distributions of individual shallow cumulus clouds in an LES, *Atmos. Chem. Phys.*, *13*, 7795–7811, doi:10.5194/acp-13-7795-2013.

De Roode, S. R., A. P. Siebesma, H. J. J. Jonker, and Y. D. Voogd (2012), Parameterization of the vertical velocity equation for shallow cumulus clouds, *Mon. Weather Rev.*, *140*, 2424–2436, doi:10.1175/MWR-D-11-00277.1.

De Rooy, W. C., and A. P. Siebesma (2008), A simple parameterization for detrainment in shallow cumulus, *Mon. Weather Rev.*, *136*, 560–576, doi:10.1175/2007MWR2201.1.

De Rooy, W. C., and A. P. Siebesma (2010), Analytical expressions for entrainment and detrainment in cumulus convection, *Q. J. R. Meteorol. Soc.*, *136*, 1216–1227, doi:10.1002/qj.640.

De Rooy, W. C., et al. (2013), Entrainment and detrainment in cumulus convection: An overview, *Q. J. R. Meteorol. Soc.*, *139*, 1–19, doi:10.1002/qj.1959.

Gregory, D. (2001), Estimation of entrainment rate in simple models of convective clouds, *Q. J. R. Meteorol. Soc.*, *127*, 53–72, doi:10.1002/qj.49712757104.

Heus, T., H. J. J. Jonker, H. E. A. Van den Akker, E. J. Griffith, M. Koutek, and F. H. Post (2009), A statistical approach to the life cycle analysis of cumulus clouds selected in a virtual reality environment, *J. Geophys. Res.*, *114*, D06208, doi:10.1029/2008JD010917.

Holtslag, A. A. M., and C.-H. Moeng (1991), Eddy diffusivity and countergradient transport in the convective atmospheric boundary layer, *J. Atmos. Sci.*, *48*, 1690–1698.

Jensen, M. P., and A. D. D. Genio (2006), Factors limiting convective cloud-top height at the ARM Nauru Island Climate Research Facility, *J. Clim.*, *19*, 2105–2117, doi:10.1175/JCLI3722.1.

Jonas, P. R. (1990), Observations of cumulus cloud entrainment, *Atmos. Res.*, *25*, 105–127, doi:10.1016/0169-8095(90)90008-Z.

Kain, J. S., and J. M. Fritsch (1990), A one-dimensional entraining/detraining plume model and its application in convective parameterization, *J. Atmos. Sci.*, *47*, 2784–2802, doi:10.1175/1520-0469(1990)047<2784:AODEPM>2.0.CO;2.

Lin, C. (1999), Some bulk properties of cumulus ensembles simulated by a cloud-resolving model. Part II: Entrainment profiles, *J. Atmos. Sci.*, *56*, 3736–3748, doi:10.1175/1520-0469(1999)056<3736:SBPOCE>2.0.CO;2.

Marsaglia, G., and T. A. Bray (1964), A convenient method for generating normal variables, *SIAM Rev.*, *6*, 260–264.

Marsaglia, G., and W. W. Tsang (2000), A simple method for generating gamma variables, *ACM Trans. Math. Software*, *26*, 363–372, doi:10.1145/358407.358414.

Neggers, R. A. J., A. P. Siebesma, and H. J. J. Jonker (2002), A multiparcel model for shallow cumulus convection, *J. Atmos. Sci.*, *59*, 1655–1668, doi:10.1175/1520-0469(2002)059\textless1655:AMMFSC\textgreater2.0.CO;2.

Neggers, R. A. J., M. Köhler, and A. C. M. Beljaars (2009), A dual mass flux framework for boundary layer convection. Part I: Transport, *J. Atmos. Sci.*, *66*, 1465–1487, doi:10.1175/2008JAS2635.1.

Park, S. (2014), A unified convection scheme (UNICON). Part I: Formulation, *J. Atmos. Sci.*, *71*, 3902–3930, doi:10.1175/JAS-D-13-0233.1.

Plank, V. G. (1969), The size distribution of cumulus clouds in representative Florida populations, *J. Appl. Meteorol.*, *8*, 46–67, doi:10.1175/1520-0450(1969)008<0046:TSDOCC>2.0.CO;2.

Rauber, R. M., et al. (2007), Rain in shallow cumulus over the ocean: The RICO campaign, *Bull. Am. Meteorol. Soc.*, *88*, 1912–1928, doi:10.1175/BAMS-88-12-1912.

Romps, D. M., and A. B. Charn (2015), Sticky thermals: Evidence for a dominant balance between buoyancy and drag in cloud updrafts, *J. Atmos. Sci.*, *72*, 2890–2901, doi:10.1175/JAS-D-15-0042.1.

Romps, D. M., and Z. Kuang (2010), Nature versus nurture in shallow convection, *J. Atmos. Sci.*, *67*, 1655–1666, doi:10.1175/2009JAS3307.1.

Siebesma, A. P., and J. W. M. Cuijpers (1995), Evaluation of parametric assumptions for shallow cumulus convection, *J. Atmos. Sci.*, *52*, 650–666, doi:10.1175/1520-0469(1995)052\textless0650: EOPAFS\textgreater2.0.CO;2.

Siebesma, A. P., et al. (2003), A large eddy simulation intercomparison study of shallow cumulus convection, *J. Atmos. Sci.*, *60*, 1201–1219.

Siebesma, A. P., P. M. M. Soares, and J. Teixeira (2007), A combined eddy-diffusivity mass-flux approach for the convective boundary layer, *J. Atmos. Sci.*, *64*, 1230–1248, doi:10.1175/JAS3888.1.

Simpson, J., and V. Wiggert (1969), Models of precipitating cumulus towers, *Mon. Weather Rev.*, *97*, 471–489, doi:10.1175/1520-0493(1969)097\textless0471:MOPCT\textgreater2.3.CO;2.

Soares, P. M. M., P. M. A. Miranda, A. P. Siebesma, and J. Teixeira (2004), An eddy-diffusivity/mass-flux parametrization for dry and shallow cumulus convection, *Q. J. R. Meteorol. Soc.*, *130*, 3365–3383, doi:10.1256/qj.03.223.

Sommeria, G., and J. W. Deardorff (1977), Subgrid-scale condensation in models of nonprecipitating clouds, *J. Atmos. Sci.*, *34*, 344–355, doi:10.1175/1520-0469(1977)034<0344:SSCIMO>2.0.CO;2.

Stevens, B., et al. (2005), Evaluation of large-eddy simulations via observations of nocturnal marine stratocumulus, *Mon. Weather Rev.*, *133*, 1443–1462, doi:10.1175/MWR2930.1.

Sušelj, K., J. Teixeira, and D. Chung (2013), A unified model for moist convective boundary layers based on a stochastic eddy-diffusivity/mass-flux parameterization, *J. Atmos. Sci.*, *70*, 1929–1953, doi:10.1175/JAS-D-12-0106.1.

Tian, Y., and Z. Kuang (2016), Dependence of entrainment in shallow cumulus convection on vertical velocity and distance to cloud edge, *Geophys. Res. Lett.*, *43*, 4056–4065, doi:10.1002/2016GL069005.

Tiedtke, M. (1989), A comprehensive mass flux scheme for cumulus parameterization in large-scale models, *Mon. Weather Rev.*, *117*, 1779–1800, doi:10.1175/1520-0493(1989)117\textless1779: ACMFSF\textgreater2.0.CO;2.

Troen, I., and L. Mahrt (1986), A simple model of the atmospheric boundary layer: Sensitivity to surface evaporation, *Bound. Layer Meteor.*, *37*, 129–148.

van Zanten, M. C., et al. (2011), Controls on precipitation and cloudiness in simulations of trade-wind cumulus as observed during RICO, *J. Adv. Model. Earth Syst.*, *3*, M06001, doi:10.1029/2011MS000056.

Vial, J., J.-L. Dufresne, and S. Bony (2013), On the interpretation of inter-model spread in CMIP5 climate sensitivity estimates, *Clim. Dyn.*, *41*, 3339–3362, doi:10.1007/s00382-013-1725-9.